Current Regulation and Fault Tolerance in Double-Delta Sourced Transformer

Yongsoon Park, Jeong-Mock Yoo, and Seung-Ki Sul
Department of Electrical and Computer Engineering
Seoul National University, Seoul, Korea

***Abstract*—The concept of Double-Delta Sourced Transformer (DDST) had been proposed to eliminate passive filters in large-scale power conversion systems. For the grid connection, active and reactive powers in DDST must be under control. In this paper, the power modulation method is proposed for DDST through the current regulation. And, it is also considered when one of converters is disconnected from the transformer. The effectiveness of the proposed method is discussed with experimental results through a proto-type set-up.**

I. INTRODUCTION

Battery Energy Storage System (BESS) is currently under consideration in Korea, in particular, for the frequency regulation [1]. An attractive point of BESS in this application is its fast response to power requirements from the grid [2]. Since this type of BESS is expected to be directly connected to distribution transformers, its power rating can be over Mega-Watt (MW) for the grid frequency regulation. A new topological study may be necessary to increase the power rating over MW, keep the conversion efficiency high, and reduce the size of BESS.

Double-Delta Sourced Transformer (DDST) had been proposed in an effort to eliminate the passive filters, whose size is physically demanding in large-scale power systems [3]. Therefore, this topology could be a potential candidate for BESS aiming the frequency regulation. Although the multilevel principle of DDST was explained in the literature, it has not been described before how active and reactive powers are modulated in DDST.

The power modulation can be achieved by regulating the converter currents in DDST. Then, the circuit modeling of DDST is described in this paper for the current regulation. If this modeling is considered at the synchronous d-q reference frame, the active power can be expressed with respect to the q-axis currents as widely known [4]. In addition, the current regulators are designed such that the regulating operation of one converter in DDST is decoupled from that of the other converter.

The fundamental operation of DDST also needs to be addressed in terms of common mode voltages and circulating currents. Because these components do not contribute to the main power transfer to the grid, they have to be minimized or nullified. The associated analyses are fully delineated and corroborated with experimental results.

One of converters in DDST might be stalled by some faults that are only confined to that abnormal converter. In this case, BESS can be operated with reduced power through the non-faulty converter. The power modulation is also discussed under this one converter operation. In addition, the harmonic properties of currents and voltages are discussed under this operation because the interleaving effect of DDST is changed.

II. DOUBLE-DELTA SOURCED TRANSFORMER

DDST originated from the conventional topology shown in Fig. 1(a) that can mitigate ripple currents at the primary side of the transformer through the interleaving of two-level converters [3]. However, since the ripple mitigation is not expected at the secondary side by the conventional wiring, large ripple currents lead to considerable losses in the converters and the secondary winding of the transformer. At the expense of DC-link sharing between the converters, DDST shown in Fig. 1(b) can reduce the ripples not only at the primary side but also at the secondary side. Because of the increased number of levels for the winding voltage through DDST wiring method, shown in Fig 2. In Fig. 2(a), only three levels are observed in the winding voltage because the line-to-line voltages of two-level converters are applied to the windings in the conventional topology. On the other hand, the voltage levels are increased up to nine by DDST as shown in Fig. 2(b). Through properly adjusting the pulse width modulation (PWM), the harmonic property by DDST is expected to be conspicuously improved.

The advantage of DDST at the harmonic property comes from combining converters and windings altogether. This combination should be carefully investigated to check whether any unnecessary current flows through windings or converters. Initially, because the common mode voltages, which conceptually include zero-sequence voltages, are inevitable at PWM, their influence of the converter should be analyzed.

978-1-4673-7151-3/15/$31.00 ©2015 IEEE

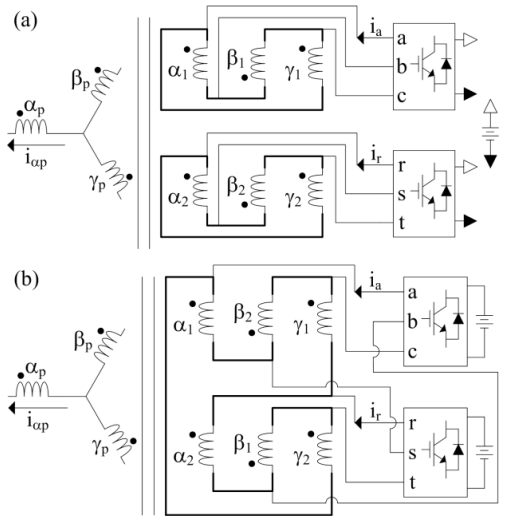

Figure 1. Interleaving operation using transformer, (a) conventional wiring, (b) DDST.

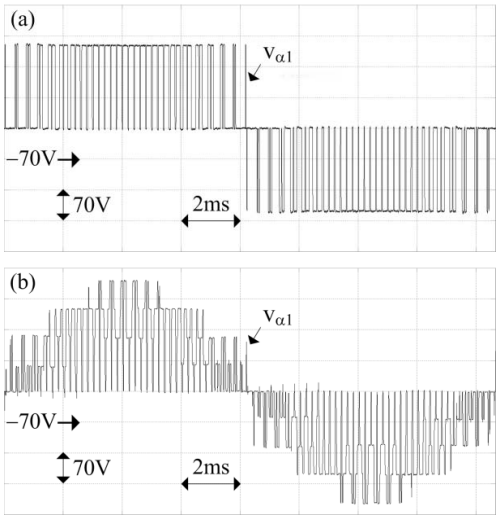

Figure 2. Winding voltage of transformer, (a) conventional wiring, (b) DDST.

According to the superposition principle, the winding voltages are derived with respect to the converter voltages from Fig. 1(b) [3]:

$$\begin{cases} v_{\alpha 1} = v_a - v_s \\ v_{\beta 1} = v_b - v_t \\ v_{\gamma 1} = v_c - v_r \end{cases} \quad (1\text{-a})$$

$$\begin{cases} v_{\alpha 2} = v_r - v_b \\ v_{\beta 2} = v_s - v_c \\ v_{\gamma 2} = v_t - v_a \end{cases} . \quad (1\text{-b})$$

It should be noticed that abc- and rst-voltages in (1) can incorporate common mode voltages. Then, three-phase voltages from the abc- and the rst-converters are given as follows.

$$\begin{cases} v_a = v_{ae} + v_{cm1} \\ v_b = v_{be} + v_{cm1} \\ v_c = v_{ce} + v_{cm1} \end{cases} \quad (2\text{-a})$$

$$\begin{cases} v_r = v_{re} + v_{cm2} \\ v_s = v_{se} + v_{cm2} \\ v_t = v_{te} + v_{cm2} \end{cases} \quad (2\text{-b})$$

,where the subscript 'cm' means common mode, and the subscript 'e' indicates the effective voltage for the current regulation without common mode components.

The common mode voltages in (2) can be separately considered from the effective voltages by the superposition principle. Thus, after inserting (2) into (1), the common mode voltages applied to the windings are derived as

$$v_{\alpha 1\_cm} = v_{\beta 1\_cm} = v_{\gamma 1\_cm} = v_{cm1} - v_{cm2} = v_{cms} \quad (3\text{-a})$$

$$v_{\alpha 2\_cm} = v_{\beta 2\_cm} = v_{\gamma 2\_cm} = v_{cm2} - v_{cm1} = -v_{cms} . \quad (3\text{-b})$$

When the secondary side windings are only concerned, the application of the common mode voltages in (3) can be understood with Fig. 3. Let us assume that non-zero currents flow according to the arrows in Fig. 3 when v_{cms} is positive. Then, all the currents at the point 'x' flow out while all the currents at the point 'y' flow into, which contradicts Kirchhoff's current law (KCL). Therefore, no current can be resulted by the common mode voltages at all in DDST.

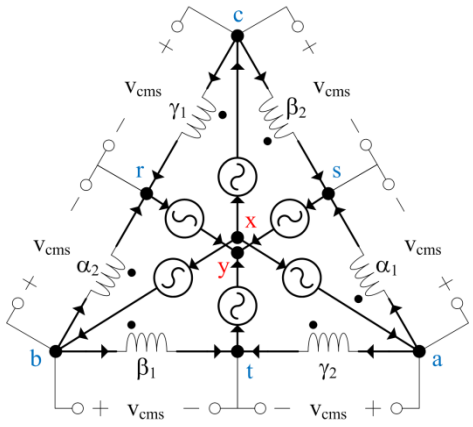

Figure 3. Transformer winding at the secondary side in DDST.

The common mode currents have been confirmed from a 6 kVA transformer (110/110V, Y-Δ) where Fig. 2 was also obtained. The respective DC-links of the converters were set to 190 V. In addition, the carrier frequency was 2.5 kHz, and the carrier waves showed 180-degree difference to each other for the interleaving. Because the common mode currents are identical for each phase in one converter, they can be observed through the sum of the three-phase current as

shown in Fig. 4, where the rated power was supplied to the grid. The common mode currents were about 0.097 A_{rms} while the converter currents were 15.4 A_{rms}. As expected, the common mode currents are rarely injected in DDST.

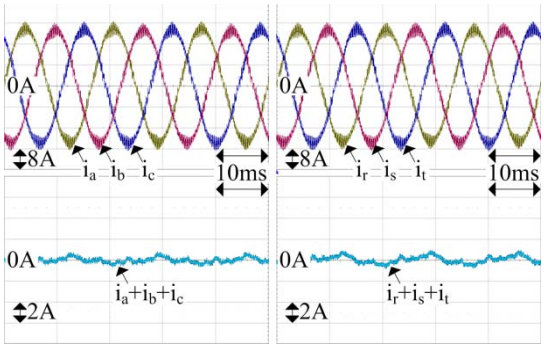

Figure 4. Common mode currents in 6 kVA transformer.

In addition to the common mode current, the circulating current should be checked in DDST where six windings form a closed loop. When considering the notation in Fig. 5, the voltage equations are derived as follows.

$$\begin{cases} v_{ae} - v_{se} = R_1 i_{\alpha 1} + L_1 \dfrac{d}{dt} i_{\alpha 1} + e_\alpha \\ v_{be} - v_{te} = R_1 i_{\beta 1} + L_1 \dfrac{d}{dt} i_{\beta 1} + e_\beta \\ v_{ce} - v_{re} = R_1 i_{\gamma 1} + L_1 \dfrac{d}{dt} i_{\gamma 1} + e_\gamma \end{cases} \quad (4\text{-a})$$

$$\begin{cases} v_{re} - v_{be} = R_2 i_{\alpha 2} + L_2 \dfrac{d}{dt} i_{\alpha 2} + e_\alpha \\ v_{se} - v_{ce} = R_2 i_{\beta 2} + L_2 \dfrac{d}{dt} i_{\beta 2} + e_\beta \\ v_{te} - v_{ae} = R_2 i_{\gamma 2} + L_2 \dfrac{d}{dt} i_{\gamma 2} + e_\gamma \end{cases} \quad (4\text{-b})$$

, where R indicates winding resistance, and L means the leakage inductance.

The effective voltages from (2) are only considered in (4) as the effect of the common mode voltages is negligible. In addition, the differentials of the flux linkages at the same limb in the transformer are assumed to be identical. This is why e_α, e_β, and e_γ are repeated in (4-a) and (4-b), which are referred as flux voltages hereafter. Because the circulating current is incorporated in all the winding currents by its definition, it can be confirmed by summing the winding currents. Then, the summation is derived as follows.

$$\begin{aligned} & i_{\alpha 1} + i_{\beta 1} + i_{\gamma 1} + i_{\alpha 2} + i_{\beta 2} + i_{\gamma 2} \\ & = \frac{1}{R_1 + sL_1}(v_{ae} + v_{be} + v_{ce} - v_{re} - v_{se} - v_{te} - e_\alpha - e_\beta - e_\gamma) \\ & + \frac{1}{R_2 + sL_2}(v_{re} + v_{se} + v_{te} - v_{ae} - v_{be} - v_{ce} - e_\alpha - e_\beta - e_\gamma) \end{aligned} \quad (5)$$

, where 's' means the Laplace operator.

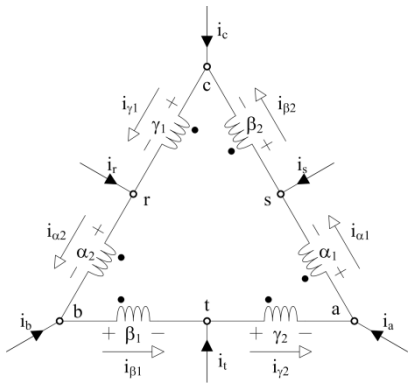

Figure 5. Currents and voltages in DDST.

The sum of the three-phase voltage from each converter is null in (5) because that is the effective three-phase voltage without the common mode voltages. Thus, the sum of the flux voltages are only the factors to cause the circulating current in (5), where the winding impedances are assumed to be identical for each three-phase winding. However, if the transformer consists of three limbs, those voltages result in the circulation current because the sum of fluxes is null and the differentiation of the sum of fluxes, which is the sum of the flux voltages, is also null. That is, no circulation current can flow if the winding impedances are balanced and the sum of the fluxes of the transformer is null.

The circulating current can be practically observed through the winding currents sorted by the subscript number in Fig. 5. Initially, the equation (6) can be derived from each node in the figure according to KCL:

$$\begin{cases} i_a = i_{\alpha 1} - i_{\gamma 2} \\ i_b = i_{\beta 1} - i_{\alpha 2} \\ i_c = i_{\gamma 1} - i_{\beta 2} \end{cases} \quad (6\text{-a})$$

$$\begin{cases} i_r = i_{\alpha 2} - i_{\gamma 1} \\ i_s = i_{\beta 2} - i_{\alpha 1} \\ i_t = i_{\gamma 2} - i_{\beta 1} \end{cases} . \quad (6\text{-b})$$

From (6), the sum of converter currents are derived as follows

$$\begin{aligned} & i_a + i_b + i_c = -(i_r + i_s + i_t) \\ & = i_{\alpha 1} + i_{\beta 1} + i_{\gamma 1} - i_{\alpha 2} - i_{\beta 2} - i_{\gamma 2} \end{aligned} . \quad (7)$$

However, because the common mode currents are negligible as shown in Fig. 4, (8) can be derived from (7):

$$i_{\alpha 1} + i_{\beta 1} + i_{\gamma 1} = i_{\alpha 2} + i_{\beta 2} + i_{\gamma 2} . \quad (8)$$

Then, the circulating current can be estimated from the winding currents as shown in Fig. 6, which was obtained under the same condition with Fig. 4. While the winding

currents were 9 A_{rms}, the circulating current was 0.15 A_{rms}. It should be noticed that third order harmonics are presented in the summations of the winding currents because of the magnetization of the transformer core. Therefore, it is ascertained that the circulating current is also negligible like the common mode currents.

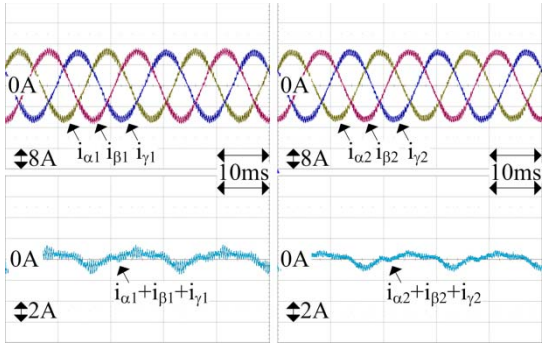

Figure 6. Circulating current in DDST.

III. Power Modulation in DDST

The winding currents are directly related to the power modulation in DDST because the power generated by the converters is transferred through the currents with respect to the flux voltages, e_α, e_β, and e_γ in (4). However, the current sensors in the converters are more practical than those in the transformer from the perspective of implementation. Thus, the power modulation should be discussed in terms of the converter currents.

The voltage equations in (4) can be rearranged into (9) by the subtractions between the winding voltage equations according to (6). All the winding impedances are assumed to be balanced, and it is used that the sum of the effective three-phase voltage is null as mentioned earlier.

$$\begin{cases} 2v_{ae}+v_{re}=Ri_a+L\dfrac{d}{dt}i_a+e_{\alpha\gamma} \\ 2v_{be}+v_{se}=Ri_b+L\dfrac{d}{dt}i_b+e_{\beta\alpha} \\ 2v_{ce}+v_{te}=Ri_c+L\dfrac{d}{dt}i_c+e_{\gamma\beta} \end{cases} \tag{9-a}$$

$$\begin{cases} 2v_{re}+v_{ae}=Ri_r+L\dfrac{d}{dt}i_r+e_{\alpha\gamma} \\ 2v_{se}+v_{be}=Ri_s+L\dfrac{d}{dt}i_s+e_{\beta\alpha} \\ 2v_{te}+v_{ce}=Ri_t+L\dfrac{d}{dt}i_t+e_{\gamma\beta} \end{cases}. \tag{9-b}$$

The right-sides of (9) are expressed with the converter currents and the line-to-line flux voltages, and the products of these variables are associated with the active and reactive powers. In addition, (9) can be transformed into the synchronous reference frame such that the component of the line-to-line flux voltages only exists in the q-axis. The transformation angle can be computed from $e_{\alpha\gamma}$, $e_{\beta\alpha}$, and $e_{\gamma\beta}$ by the phase locked loop (PLL) [5], [6]. Then the voltage equation at the synchronous reference frame can be derived as follows.

$$\begin{bmatrix} v_{ds1} \\ v_{qs1} \end{bmatrix}=\begin{bmatrix} R & -\omega L \\ \omega L & R \end{bmatrix}\begin{bmatrix} i_{d1} \\ i_{q1} \end{bmatrix}+L\frac{d}{dt}\begin{bmatrix} i_{d1} \\ i_{q1} \end{bmatrix}+\begin{bmatrix} 0 \\ E \end{bmatrix} \tag{10-a}$$

$$\begin{bmatrix} v_{ds2} \\ v_{qs2} \end{bmatrix}=\begin{bmatrix} R & -\omega L \\ \omega L & R \end{bmatrix}\begin{bmatrix} i_{d2} \\ i_{q2} \end{bmatrix}+L\frac{d}{dt}\begin{bmatrix} i_{d2} \\ i_{q2} \end{bmatrix}+\begin{bmatrix} 0 \\ E \end{bmatrix} \tag{10-b}$$

$$\begin{bmatrix} v_{ds1} \\ v_{qs1} \\ v_{ds2} \\ v_{qs2} \end{bmatrix}=\begin{bmatrix} 2 & 0 & 1 & 0 \\ 0 & 2 & 0 & 1 \\ 1 & 0 & 2 & 0 \\ 0 & 1 & 0 & 2 \end{bmatrix}\begin{bmatrix} v_{d1} \\ v_{q1} \\ v_{d2} \\ v_{q2} \end{bmatrix} \tag{10-c}$$

, where i_{d1} and i_{q1} are the synchronous d-q current from the abc-current while i_{d2} and i_{q2} from the rst-current. Similarly, v_{d1} and v_{q1} are the synchronous d-q voltage from the effective abc-voltage while v_{d2} and v_{q2} from the effective rst-voltage. The magnitude of the line-to-line flux voltage is denoted as E.

The voltage outputs of each converter practically affect the other converter's currents as shown in (9). However, when considering v_{ds1}, v_{qs1}, v_{ds2}, and v_{qs2} in (10), the current regulations can be independently dealt with as per converters. Namely, i_{d1} and i_{q1} from the abc-current are only affected by v_{ds1} and v_{qs1} while i_{d2} and i_{q2} from the rst-current by v_{ds2} and v_{qs2}. This decoupling effect could be used to implement the current regulations through the inverse transformation of (10-c), which corresponds to (11). After the intermediate voltages are determined from the current regulators according to (10-a) and (10-b), the actual voltages for each converter, v_{d1}, v_{q1}, v_{d2}, and v_{q2}, can be obtained by (11). Because it is well known in the literature how the current regulator can be designed for the systems such as (10-a) and (10-b) [7], the design of the current regulator is not detailed further in this paper.

$$\begin{bmatrix} v_{d1} \\ v_{d2} \\ v_{q1} \\ v_{q2} \end{bmatrix}=\frac{1}{3}\begin{bmatrix} 2 & -1 & 0 & 0 \\ -1 & 2 & 0 & 0 \\ 0 & 0 & 2 & -1 \\ 0 & 0 & -1 & 2 \end{bmatrix}\begin{bmatrix} v_{ds1} \\ v_{ds2} \\ v_{qs1} \\ v_{qs2} \end{bmatrix}. \tag{11}$$

In fact, it is essential to detect the phase of the flux voltages for the implementation of the current regulators at the synchronous reference frame. Initially, those voltages cannot be directly measured at the secondary side, where the winding voltages are explicitly determined by the converters as shown in Fig. 1(b). Moreover, the measurement at the primary side, which is the high-voltage side of a distribution transformer in BESS, may be also difficult due to insulation issue. Thus, the tertiary winding is deemed an alternative to monitor the flux voltages. Since this tertiary winding is just to observe the differential of flux linkage at each limb, no

current needs to flow. If the current flowing in the tertiary winding is not negligible, it may cause undesirable effects from the leakage inductances of tertiary winding itself [8], [9].

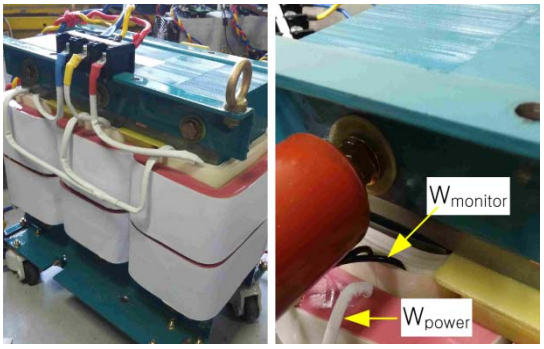

Figure 7. 6 kVA transformer for DDST.

The tertiary winding of 6 kVA transformer is indicated by $W_{monitor}$ in Fig. 7. This monitoring winding could be thinner than the main power winding, W_{power}, and was separated phase by phase not to form any loop. In addition, it is desirable that the PLL method has the filtering function to harmonics such as Second Order Generalized Integrator (SOGI) based PLL. Because the flux voltages at $W_{monitor}$ may have some pulse-width modulated components.

As mentioned earlier, the products of the flux voltages and the currents are related to the power transfer. This does at the synchronous reference frame as well. In particular, the q-axis products are meaningful in (10) because the d-axis flux voltages are null. In that both the converter currents and the line-to-line flux voltages in (9) are $\sqrt{3}$ times larger than the winding currents and the flux voltages in (4), respectively, the active power, P_{DDST}, can be derived as (12), which presents the ratio difference by 3 to the conventional power equation in the synchronous reference frame [10].

$$P_{DDST} = \frac{1}{2} \cdot E \cdot (i_{q1} + i_{q2}) . \quad (12)$$

It is notified from (12) that the active power from each converter depends on its own q-axis current in DDST. That is, the active power flow can be asymmetric between the converters by adjusting the q-axis currents. However, in the view point of the interleaving through the transformer, it would be better to make the active power balanced.

Another 5 kVA transformer (220/55V, Δ-Δ) was tested to verify the proposed power modulation. The DC-link voltages of the converters were set to 100 V, and the carrier frequency for PWM was 3.75 kHz. All control algorithms were implemented with a DSP board based on TMS320C28346.

The experimental result related to the rated active power is shown in Fig. 8. The d-q current has been captured only for the abc converter because that for the rst converter was the same. The q-axis currents were regulated as 37 A while the d-axis currents as 0 A, which intended the reactive power to be null. As shown in Fig. 8, the A-phase current to the grid, i_{ag}, lags behind the line-to-line grid voltage, v_{ab}, by 1.37 ms, which corresponds to the phase of 29.6 ° in terms of 60 Hz. Then, by considering the phase difference of the phase voltage to the line-to-line voltage, it is corroborated that the power factor was almost unity as intended. Thus, the active power to the grid was 5.15 kW since i_{ag} was 19.1 A at the grid frequency. Meanwhile, the total harmonic distortion (THD) of i_{ag} was relatively high in that it was 11.9 % at the rated power. However, it should be considered that the leakage impedance of the transformer under test was 0.032 p.u. Since the leakage impedance is expected to be 0.06 p.u. in MW-scale transformers, the harmonic distortions would be much reduced in large-scale BESSs.

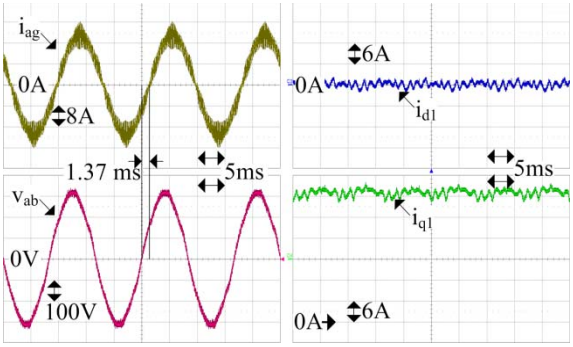

Figure 8. Currents when the rated active power is supplied to the grid.

The active power from each converter may be asymmetric as shown in Fig. 9, where the abc converter supplied its rated active power while the rst converter its half-rated active power. Namely, the A-phase converter currents, i_a and i_r, were different according to their references in the q-axis. In result, under the unity power factor, i_{ag} at the grid frequency was 14.6 A, which was close to 75 % of that in Fig. 8 as expected. Therefore, it is corroborated with Figs. 8 and 9 that the active powers of the converters are separately modulated by adjusting the q-axis current of each converter according to (12).

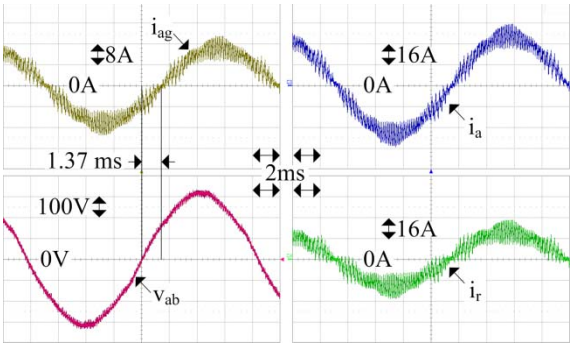

Figure 9. Asymmetric active powers from converter.

The reactive power can be modulated through the d-axis currents. This should be understood with spatial explanations rather than an equation like (12). As shown in Fig. 10, a non-zero d-axis current can particularly modify the angle of the

current vector in the synchronous reference frame. This sort of modification causes the power factor to vary since the vector angle of the flux voltage is aligned with the q-axis by the PLL. For example, if the power is transferred from the converters to the grid, a negative d-axis current means leading power factor while a positive d-axis current means lagging power factor. This fact is confirmed with Figs. 11 and 12, where the signs of d-axis currents are opposite when the magnitudes of d-axis and q-axis currents are, respectively, 20 % and 70 % of the rated current. Depending on the d-axis current, the phase of i_{ag} obviously leads or lags with respect to the point U, which indicates the unity power factor. Therefore, it depends on the signs of the d-axis currents whether the reactive power is inductive or capacitive. Needless to say, the amount of reactive power is proportional to the d-axis currents as the case of active power.

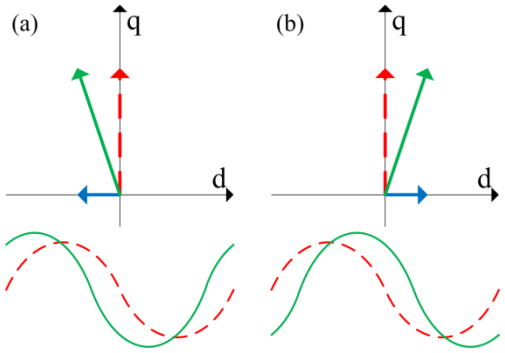

Figure 10. Phase shifts by d-axis currents: (a) leading, (b) lagging.

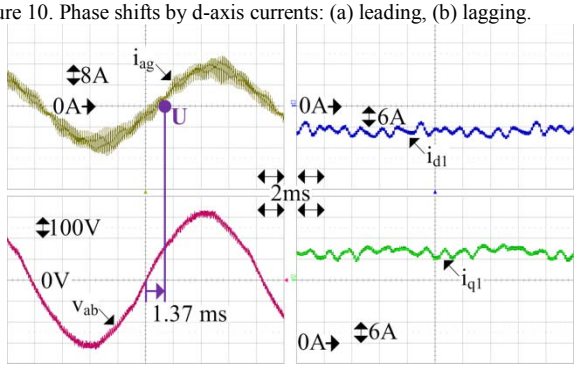

Figure 11. Leading power factor by negative d-axis current.

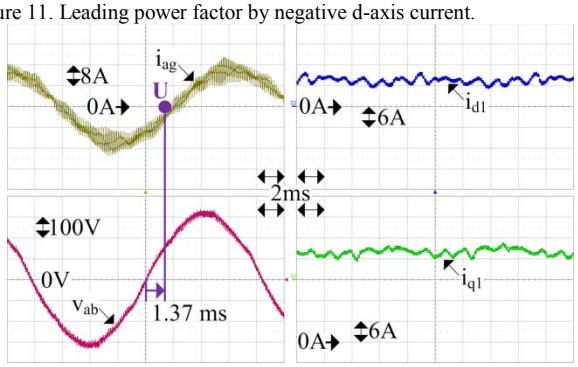

Figure 12. Lagging power factor by positive d-axis current.

IV. Fault Operation in DDST

The power transfer should be maintained even if one of the converters is dropped out by some faults in DDST. For that instance, the currents and the voltages are shown in Fig. 13 when the rst converter is disconnected. Then, the voltage equation can be derived as (13) from Fig. 13.

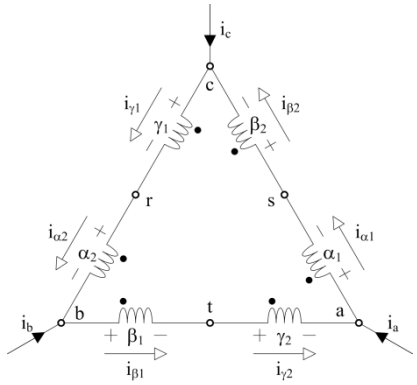

Figure 13. Currents and voltages under the fault operation.

$$\begin{cases} v_{ae} - v_{ce} = 2Ri_{\alpha 1} + 2L\dfrac{d}{dt}i_{\alpha 1} + e_{\alpha} + e_{\beta} \\ v_{be} - v_{ae} = 2Ri_{\beta 1} + 2L\dfrac{d}{dt}i_{\beta 1} + e_{\beta} + e_{\gamma} \\ v_{ce} - v_{be} = 2Ri_{\gamma 1} + 2L\dfrac{d}{dt}i_{\gamma 1} + e_{\gamma} + e_{\alpha} \end{cases} \quad (13)$$

The remaining converter can maintain the same DC-link voltage in spite of the other converter's disconnection. This is because the sum of the flux voltages in (13) only results in a phase shift of the flux voltage. For example, the sum of e_{α} and e_{β} is equal to $-e_{\gamma}$. (9), Eq. (13) can be rearranged into (14) to deal with the converter currents.

$$\begin{cases} 3v_{ae} = 2Ri_a + 2L\dfrac{d}{dt}i_a + e_{\alpha\gamma} \\ 3v_{be} = 2Ri_b + 2L\dfrac{d}{dt}i_b + e_{\beta\alpha} \\ 3v_{ce} = 2Ri_c + 2L\dfrac{d}{dt}i_c + e_{\gamma\beta} \end{cases} \quad (14)$$

As shown in (14), the winding impedances are physically doubled due to the series connections. However, (14) can be transformed into (15) by the coordinate transformation.

$$\begin{bmatrix} v_{ds1} \\ v_{qs1} \end{bmatrix} = \begin{bmatrix} R & -\omega L \\ \omega L & R \end{bmatrix}\begin{bmatrix} i_{d1} \\ i_{q1} \end{bmatrix} + L\frac{d}{dt}\begin{bmatrix} i_{d1} \\ i_{q1} \end{bmatrix} + \frac{1}{2}\begin{bmatrix} 0 \\ E \end{bmatrix} \quad (15\text{-a})$$

$$\begin{bmatrix} v_{d1} \\ v_{q1} \end{bmatrix} = \frac{2}{3}\begin{bmatrix} v_{ds1} \\ v_{qs1} \end{bmatrix}. \quad (15\text{-b})$$

Because the system equation in (15-a) is equal to (10-a) except the flux voltage, the proportional and integral gains

can be identical for the current regulators regardless of the single converter operation due to the fault [7]. In fact, the difference of the flux voltage can be naturally compensated by the integrator for the current regulation. Furthermore, when it comes to v_{d1} and v_{q1}, (15-b) coincides with (11) if v_{ds2} and v_{qs2} are ignored. That is, the design based on (15) can keep the consistency in the current regulation before and after the single converter operation. However, it should be reminded that (15-a) is a fictitious system for the current regulation. Unlike (15-a), since the actual flux voltages are not halved under the single converter operation, the active power has to be expressed with (12) by making the q-axis current of the disconnected converter null.

The current regulation under the single converter operation can be compared with Fig. 14. Even though the abc converter regulates its current, i_a, to the rated value, the grid current, i_{ag}, decreases by half under the operation. That is, the maximum power decreases by 50 % according to (12) because one of the q-axis currents must be zero under the fault operation.

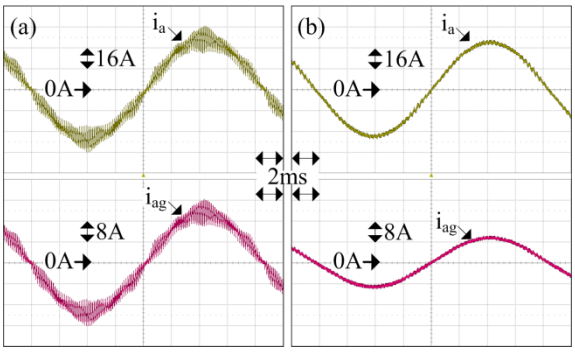

Figure 14. Converter current and grid current: (a) normal operation, (b) single converter operation.

Meanwhile, the harmonic distortions of the currents are conspicuously improved in Fig. 14(b). Namely, the THD of i_a is changed from 11.9 % to 2.5 % while i_{ag} from 12 % to 3.6 %. Even if the intended converter combination is not kept because of the fault, the interleaving effect can be continued by the winding structure of DDST it self. Initially, if one converter is dropped out as shown in Fig. 13, the remaining converter cannot strictly define every node's potential. For instance, the potential of the r-node is not simply determined by v_{cb}. This is because the winding of α_2 is magnetically coupled with the winding of α_1 while γ_1 with γ_2. That is, that potential is simultaneously affected by all the voltage outputs of the remaining converter.

The winding voltages are shown in Figs. 15 and 16 to show the difference between dual converter operation and single converter operation, which have been captured from the experiments of Figs. 14(a) and (b), respectively. Like Fig. 2(b), the number of the voltage levels is nine in Fig. 15 for the winding voltage of α_1. However, as shown in Fig. 16, the voltage level of the discrete pulse is still nine but the discrete voltage is on the top of the sinusoidal voltage. And, THD of the voltage in Fig. 16 is much less compared to that in Fig. 16. This contributes to the reduction of ripple currents at the converter side. In Figs. 15 and 16, the sum of $v_{\alpha 1}$ and $v_{\alpha 2}$ is also presented. This summation is useful to indirectly confirm the interleaving effect at the grid side in that the fluxes caused by $v_{\alpha 1}$ and $v_{\alpha 2}$ are superimposed through the same limb of the transformer. When compared to Fig. 15, this summation voltage is quite sinusoidal in Fig. 16. Therefore, it is inferred that the good quality of the currents in Fig 14(b) originates from the interleaving effect different to that under the normal operation.

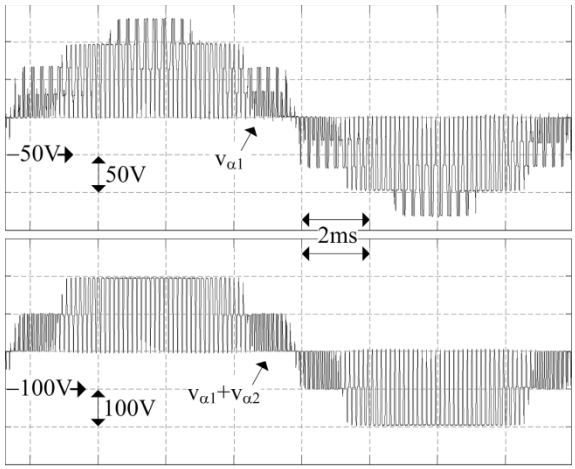

Figure 15. Winding voltages under normal operation.

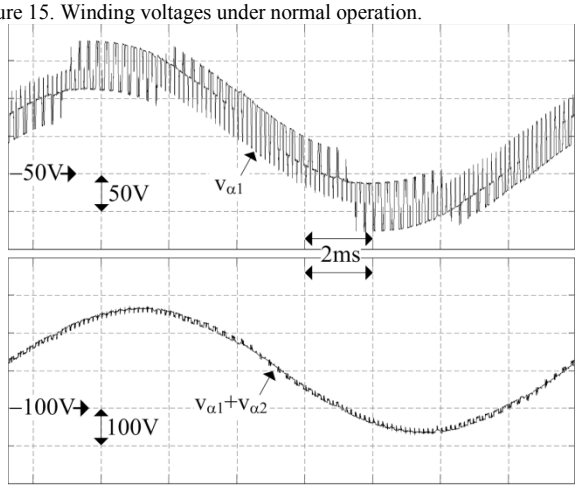

Figure 16. Winding voltages under single converter operation.

It is notable that the turn number of windings is doubled to handle the same flux voltage under the fault operation as shown in (14). This is why the maximum power becomes halved in the same transformer. Thus, normally, it is not always desirable to decrease the utilization factor of the windings in the aspect of power conversion. However, the drop in the utilization factor is inevitable under the single converter operation in DDST, and the interleaving effect presented in Fig. 16 is deemed as a natural trade-off for the power drop. This additional benefit is very helpful to comply

with the harmonic regulations even in the case of the fault [11].

V. CONCLUSION

In this paper, the fundamental operations of DDST have been discussed. Above all, the method to adjust active and reactive powers has been described and verified through experimental results. This method is based on the current regulators at the synchronous reference frame, which is separately implemented for each converter through the decoupled modeling. In addition, it has been analyzed why the undesirable currents such as common mode currents and circulating currents are negligible in DDST. Finally, the fault operation, where one of the converters is disconnected, has been addressed in terms of the power modulation and the harmonic distortions. Under the single converter operation due to the fault, DDST can deal with the half-rated power at most while retaining the interleaving effect through its own winding structure.

REFERENCES

[1] M. D. Castillo, G. P. Lim, Y. Yoon, B. Chang, "Application of Frequency Regulation Control on the 4MW/8MWh Battery Energy Storage System (BESS) in Jeju Island, Republic of Korea," *J. Energy Power Sources*, vol. 1, no. 6, pp. 287-295, Dec. 2014.

[2] K. Vu, R. Masiello, and R. Fioravanti, "Benefits of Fast-Response Storage Devices for System Regulation in ISO Markets," *Power & Energy Sosiety General Meeting, IEEE*, pp. 1-8, 26-30 July 2009.

[3] Y. Park, S. Ohn, and S.-K. Sul, "Multi-Level Operation with Two-Level Converters Through a Double-Delta Source Connected Transformer," *Journal of Power Electron.*, vol. 14, no. 6, pp 1093-1099, Nov. 2014.

[4] J.-W. Choi, and S.-K. Sul, "Fast Current Controller in Three-Phase AC/DC Boost Converter Using d-q Axis Crosscoupling," *IEEE Trans. Power Electron.*, vol. 13, no. 1, pp. 179-185, Jan. 1998.

[5] S.-K. Chung, "A Phase Tracking System for Three Phase Utility Interface Inverters", *IEEE Trans. Power Electron.*, vol. 15, no. 3, pp. 431-438, May 2000.

[6] Y. Park, S.-K. Sul, W.-C. Kim, and H.-Y. Lee, "Phase-Locked Loop Based on an Observer for Grid Synchronization," *IEEE Trans. Ind. Appl.*, vol. 50, no. 2, pp. 1256-1265, Mar./Apr. 2014.

[7] S.-K. Sul, "Design of regulators for electric machines and power converters", *in Control of Electric Machine Drive Systems*, Hoboken, NJ: Wiley, ch. 4, pp. 154-282, 2011.

[8] M. Lambert, M. Martinez-Duro, J. Mahseredjian, F. D. Leon, and F. Sirois, "Transformer Leakage Flux Models for Electromagnetic Transients: Critical Review and Validation of a New Model," *IEEE Trans. Power Delivery*, vol. 29, no. 5, pp. 2180-2188, Oct. 2014.

[9] F. D. Leon, and J. A. Martinez, "Dual Three-Winding Transformer Equivalent Circuit Matching Leakage Measurements", *IEEE Trans. Power Delivery*, vol. 24, no. 1, pp. 160-168, Jan. 2009.

[10] D. W. Novotny, and T. A. Lipo, "Power Flow in the d,q Equivalent Circuit", *in Vector Control and Dynamics of AC Drives*, NY: Oxford Univ. Press Inc., ch. 2.10, p. 69, 1996.

[11] *IEEE Standard for Interconnecting Distributed Resources With Electric Power Systems*, IEEE Std. 1547, 2003.